

I. Determination of chemical reaction rate constants by numerical nonlinear analysis: differential methods

Christopher G. Jesudason *

Department of Chemistry and Center for Theoretical and Computational Physics
University of Malaya
50603 Kuala Lumpur, Malaysia

January 27, 2011

Abstract

The primary emphasis of this work on kinetics is to illustrate the *a posteriori* approach to applications, where focus on data leads to novel outcomes, rather than the *a priori* tendencies of applied analysis which imposes constructs on the nature of the observable. The secondary intention is the development of appropriate methods consonant with experimental definitions. Chemical kinetic equations were largely developed with the assumption of rate constant invariance and in particular rate constant determination usually required knowledge of the initial concentrations. These methods could not determine the instantaneous rate constant. Previous work based on precise simulation data [J. Math . Chem **43** (2008) 976–1023] of a bidirectional chemical reaction system in equilibrium concluded that the rate constants is a function of species concentration through the defined and determined reactivity coefficients for at least elementary reactions. Inhomogeneities in the reaction medium might also lead to cross-coupling of forces and fluxes, leading to concentration dependencies. By focusing on gradients, it is possible to determine both the average and instantaneous rate constants that can monitor changes in the rate constant with concentration changes as suggested by this theory. Here, methods are developed and discussed utilizing nonlinear analysis which does not require exact knowledge of initial concentrations. These methods are compared with those derived from standard methodology for known chemical reactions studied by eminent kineticists and in one case with a reaction whose initial reactant concentration was not well determined. These gradient methods are shown to be consistent with the ones from standard methods and could readily serve as alternatives for studies where there are limits or unknowns in the initial conditions, such as in the burgeoning fields of astrophysics and astrochemistry, forensics, archeology and biology . All four reactions studied exhibited semi sinusoidal-like change with reactant concentration change which standard methods cannot detect, which

*Emails: jesu@um.edu.my or chris_guna@yahoo.com

seems to constitute the observation of a new effect that is not predicted by current formulations, where the possibility that the observations are due to artifacts from instrumental errors or the optimization method is reasoned as unlikely since the experiments were conducted by different groups at very different times with different classes of reactions. Two broad reasons are given for this observation, and experiments are suggested that can discriminate between these two effects. Although first and second order reactions were investigated here using data from prominent experimentalists, the method applies to arbitrary fractional orders by polynomial expansion of the rate decay curves where closed form integrated expressions do not exist. Integral methods for the above will be investigated next.

Keywords: numerical nonlinear analysis; orthogonal polynomial expansion; chemical reaction rate law; *a priori*; *a posteriori*

1 INTRODUCTION AND METHODS

Current trends in mathematical applications almost always indicate the creation of mathematical structures that are then supposed and considered to mirror physical reality and experimental outcomes. Less common are applications that analyze experimental data using as closely as possible the operational definition of variables to elucidate the validity or otherwise of theories. The main thrust of this sequel is to illustrate research that puts priority on the experimental data as a means to constructing or suggesting theoretical and mathematical structures. The data from highly empirical field of chemical kinetics is used within the scope of the definition of the measured variables to discover/uncover new effects; it is suggested here based on the outcome of the analysis that mathematical analysis of the data in other fields within the operational definition of the empirical variables can elucidate new phenomena and suggest how appropriate and consistent theory can be constructed *a posteriori*, rather than the *a priori* tendencies of many applied mathematicians. One aspect of this culture is the cult of prediction and of predictability in the natural sciences where resources are expended in performing experiments to verify and substantiate theories. The methods developed here are of secondary importance compared to the *a posteriori* analysis of the data and its outcomes; these methods refer to variables which come from the experimental definition. For an elementary reaction



we define the rate constant k as the factor in the equation

$$\frac{d[A_1]}{dt} = [\dot{A}] = -k[Q] \quad (2)$$

where

$$[Q] = \prod_{i=1}^{n_r} [A_i]^{\nu_i} = l_{A_1 A_2 \dots A_{n_r}}(t) = l_Q(t)$$

with $l_R(t) = [R](t)$ in general and $l_A(t) = [A]_1(t)$ in particular, with the notation $l_{A_1}(t)l_{A_2}(t) \dots l_{A_{n_r}}(t) = l_Q(t)$. The square brackets denote the concentration of the

species, and t is the time parameter. For the above, the order O , which need not be integer is defined as $O = \sum_{i=1}^{n_r} \nu_i$. Clearly, for the above

$$k = - \left\{ \frac{d[A_1]}{dt} \right\} / Q. \quad (3)$$

We determine k here directly by various methods of computing average and instantaneous gradients for equation (2). In traditional methods, the integrated rate law expression is known for only a handful of integer O values of (2) which also require initial conditions; no such restrictions apply to the current numerical technique. Another class of method is through a least squares optimization of the function $R(k)$ for n datapoints defined as

$$R(k) = \sum_{i=1}^n \left(\frac{dl_A(t_i)}{dt} - kl_Q(t_i) \right)^2. \quad (4)$$

Then,

$$R'(k) = 0 \Rightarrow \sum_{i=1}^n \left(\frac{dl_A(t_i)}{dt} - kl_Q(t_i) \right) l_Q(t_i) = 0$$

implies

$$k = - \frac{\sum_{i=1}^n \frac{dl_A(t_i)}{dt} \cdot l_Q(t_i)}{\sum_{i=1}^n l_Q^2(t_i)}. \quad (5)$$

Eq.(5) does not require iterative methods such as Newton-Raphson's (NR) to determine the rate constant. A variant of the $R(k)$ optimization above is found in Sec(2.0.5); the reason being that we optimize over an integrated expression rather than directly the rate equation (2) such as (18) for the first order rate constant k_1 and 19 for the second order constant k_2 . All variants of the above methods will be discussed in sequence in what follows. Most kinetic determinations use logarithmic plots with known initial concentrations, although there have been attempts at integral methods [1, 2, 3, 4, 5, 6, 7, 8, 9, 10, 11, 12, and refs. therein] that dispense with the initial concentration. (There may be ambiguities in e.g. [1] concerning choice of independent variables that will be discussed elsewhere). These standard methods all assume constancy of the rate constant k , and therefore have not inspired methodology that can detect the changes to the rate constant that, according to the detailed results of ref.[13] sheds important information on the activation energy profile changes due to the force fields acting on the reacting species. There are conceivably many other reasons for variation with time of the rate constants; they include coupling of inhomogenous temperature field gradients with chemical species fluxes, leading to physical variable inhomogeneities in the reaction cell that modifies the rate of reaction with time. This is discussed after the data is presented in what follows.

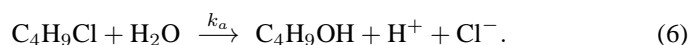
There have been detailed and specialized reports and treatises of computational techniques over the many decades but these have been sparse and far between. Wiberg has [14, p.757] described various more advanced series expansion techniques in conjunction with least squares analysis to derive kinetic data. His use of numerical integration is confined to solving by Runge-Kutta integration a set of coupled equations, such as feature in an enzyme-catalysed reaction [14, p.771]. Wiberg in turn draws upon

the collective efforts collated by D. F. Detar [15, 16]. It seems that Detar's collation anticipates to some degree many of the developments cited above in this work's bibliography. A first order treatment of a chemical reaction is given in the program LSKIN1 [15, p.126] requires data and time intervals that are conformable to the Roseveare-Guggenheim time interval requirement. LSKIN2 [16, p.3] solves for rate constant and initial concentrations of a second order reaction based on a series expansion of the integrated rate law expression. Here, the curvature would introduce "errors" if a linear expansion were used. For both these methods, the constancy of the rate constant k is a basic assumption, which is not the case here.

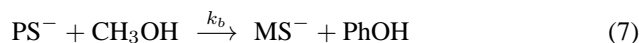
Nonlinear analysis (NLA), will be attempted here in preliminary form, in order to compute both the instantaneous and average rate constants. We analyze 2 first order reactions and one second order one using data from prominent kineticists. In addition, we select one first order reaction whose initial concentration index is ambiguous utilizing the others as a reference to gauge the likelihood of our result based on NLA; if our analysis concurs with the 3 reactions from the literature, then one might be confident that the NLA analysis of the ambiguous reaction is reasonably accurate. Important experiments in science are conducted under uncontrolled conditions, such as in astrochemical reaction rate determinations and photochemical emission spectra in the Mars and Titan atmospheres over the several decades [17, 18, 19]. A similar situation obtains in forensic science and archeology and in biological physiological rate determinations. The basic methods presented here caters for both controlled and uncontrolled initial conditions.

The 3 first order reactions (i)-(iii) and second order reaction (iv) studied are itemized below:

- (i) the tert butyl chloride hydrolysis reaction in ethanol solvent (80% v/v) at 25°C derived from the Year III teaching laboratory of this University (UM) where the initial concentration, although determined, is ambiguous. Because of time constraints, the inaccurate $\lambda_{\infty} = 2050 \mu\text{S cm}^{-1}$ for (i) was determined by heating the reaction vessel at the end of the monitoring to 60°C until there was no apparent change in the conductivity when equilibrated back at 25°C. Reaction (i) involved 0.3mL of the reactant which was dissolved in 50mL of ethanol initially. The reaction was conducted at 25°C and monitored over time (minutes) by measuring conductivity ($\mu\text{S cm}^{-1}$) due to the release of H^+ and Cl^- ions as shown below in (6),



- (ii) the methanolysis of ionized phenyl salicylate derived from the literature [20, Table 7.1, p.381] with presumably accurate values of both the initial concentration and for all data sets of the kinetic run. Reaction (ii) may be written



where for the rate law is pseudo first-order expressed as

$$\text{rate} = k_b[\text{PS}]^- = k_c[\text{CH}_3\text{OH}][\text{PS}^-].$$

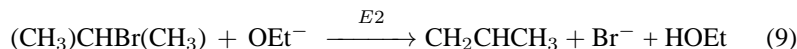
The methanol concentration is in excess and is effectively constant for the reaction runs [20, p.407]. The data for this reaction is given in detail in [20, Table 7.1], conducted at 30°C where several ionic species are present in the reaction solution from KOH, KCl, and H₂O electrolytes.

- (iii) the primarily SN1 substitution reaction [25, Table IX,p.2071] of tertiary butyl bromide (Bu^tBr) with dilute ethyl alcoholic sodium ethoxide in ethanol solvent where there concurrently occurs an approximately 20% contribution of an E1 elimination reaction. Reaction (iii) may be written



where the solvent was EtOH with initial sodium ethoxide concentration [NaOEt] = 0.02386N at 25°C. The products consisted of approximately 81% substituted tertiary butyl ethoxide and 19% olefinic molecules due to E1 elimination. Hence the rate constant here refers to a composite reaction (details in [23, 2064] and [25, p.2070].

- (iv) the second order E2 elimination reaction [23, p.2059-2060 and Table VII,p.2064] with reactants isopropyl bromide (PrⁱBr) and sodium ethoxide (NaOEt). Reaction (iv) involving isopropyl bromide PrⁱBr \equiv (CH₃)CHBr(CH₃) may be written



where the isopropyl bromide reacts with the OEt⁻ ion in EtOH solvent at 25°C to yield 80.3% of the olefinic product with some SN2 substitution with the (OEt) functional group [23, Table III,p.2061] according to the kineticists. Further details and data appear [23, Table VII,p.2064]. It should be mentioned that the E2 reaction was inferred to be second order from prior experimental considerations since the [NaOEt] concentration reduction from the data exactly coincides with the reduction of PrⁱBr and was not independently determined. This perhaps somewhat experimentally questionable technique may well be the reason for the instantaneous rate constant as computed here to be somewhat non-smooth, as will be discussed later (see Fig.(21) for the graph).

“Units” in the figures and text pertain to the appropriate reaction variable dimension, for instance either the absorbance for (i) or the conductivity ($\mu\text{S cm}^{-1}$) for (ii) below. Either because of evaporation or the temperatures not equilibrating after heating, the measured λ_∞ , it would be inferred that for (i) the measured value is larger than the actual one determined from the analysis. Reaction (ii) is very rapid compared to (i) and the experimental data plots show high nonlinearity. We denote by λ the measurement parameter which is the conductivity $\mu\text{S cm}^{-1}$ or absorbance A [20, eqn 7.24-7.26] for reactions (i) and (ii) respectively; λ also refers to the concentration [X] of species X for reactions (iii) and (iv). The more accurately determined $\lambda_\infty = A_\infty$ for (ii) [20, Table 7.1,p.381] was at approximately 0.897. Analysis of (ii) give values of $A_\infty = \lambda_\infty$ very close to the experimental ones that suggests that our determination for reaction (i) λ_∞ is correct. The experimental data and number of readings for

the determination of rate constants is always related to the method used and the order of accuracy required in the study; for Khan [20, Table 7.1, first A column], (reaction (ii)), 14 normal readings over 360 seconds (s) sufficed for Khan's purposes, whereas for the practical class (reaction (i)), 36 readings over 55 minutes (mins) were taken. The meager 14 readings of (ii) covered a major portion of the nonlinear region of the reaction, whereas for (i) the many readings were confined to the near-linear regime. Linear proportionality is assumed between λ and the extent of reaction x , where the first order law (c being the instantaneous concentration, k the general rate constant and a the initial concentration) is $\frac{dc}{dt} = -kc = -k(a - x)$; with $\lambda_\infty = \alpha a$, $\lambda_t = \alpha x$ and $\lambda(0) = \lambda_0 = \alpha x_0$, integration yields for assumed constant k

$$\ln \frac{(\lambda_\infty - \lambda_0)}{(\lambda_\infty - \lambda(t))} = kt \quad (10)$$

Eqn.(10) determines k if λ_0 and λ_∞ are known.

The analysis for the latter reactions (ii)-(iv) would provide a reference and indication of the predicted value in (i) for the initial concentration, apart from checking for overall consistency of the methodology in general situations especially when there is doubt concerning the value of the initial concentration.

The methods presented here applies to any order provided the expressions can be expanded as an n -order polynomial of the concentration variable against the time independent variable. To get smooth curves that are stable one had to modify and use a proper curve-interpolation technique that is stable which does not form sudden kinks or points of inflexion and this follows next.

1.1 Orthogonal polynomial stabilization

It was discovered that the usual least squares polynomial method using Gaussian elimination [21, Sec.6.2.4,p.318] to derive the coefficients of the polynomial was highly unstable for $n_{poly} > 4$, which is a known condition [21, p.318, Sec 6.2.4]. For higher orders, there is in addition the tendency to form kinks and loops in an interpolated curve for values between two known intervals. Other methods described in specialized treatises [22, Ch.5, Sec.5.7-5.13], even if robust and stable, such as the Chebyshev approximation required values of the proposed experimental curve at predetermined definite points in time, which is outside the control of one using predetermined data and so for this work, the least square approximation was stabilized by orthogonal polynomials [21, Sec.6.3] modified for determination of differentials. It is hoped that the method can also be extended to integrals in future investigations. The usual method defines the n^{th} order polynomial $p_n(t)$ which is then expressed as a sum of square terms over the domain of measurement to yield Q in (11).

$$\begin{aligned} p_n(t) &= \sum_{j=0}^n h_j t^j \\ Q(f, p_n) &= \sum_{i=1}^N [f_i - p_n(t_i)]^2 \end{aligned} \quad (11)$$

The Q function is minimized over the polynomial coefficient space. In the orthogonal method adopted here, we express our polynomial expression $p_m(t)$ linearly in

coefficients a_j of φ_j functions that are orthogonal with respect to an *inner* product definition. For arbitrary functions f, g , the inner product (f, g) is defined below, together with properties of the φ_j orthogonal polynomials:

$$\begin{aligned} (f, g) &= \sum_{k=1}^N f(t_k) \cdot g(t_k) \\ (\varphi_i, \varphi_j) &= 0 \quad (i \neq j) \quad \text{and} \quad (\varphi_i, \varphi_i) \neq 0. \end{aligned} \quad (12)$$

$$\begin{aligned} \varphi_i(t) &= (t - b_i)\varphi_{i-1}(t) - c_i\varphi_{i-2}(t) \quad (i \geq 1), \\ \varphi_0(t) &= 1, \text{ and } \varphi_j = 0 \text{ for } j < 1, \\ b_i &= (t\varphi_{i-1}, \varphi_{i-1})/(\varphi_{i-1}, \varphi_{i-1}) \quad (i \geq 1), b_i = 0 \quad (i < 1), \\ c_i &= (t\varphi_{i-1}, \varphi_{i-2})/(\varphi_{i-2}, \varphi_{i-2}) \quad (i \geq 2), \text{ and } c_i = 0 \quad (i < 2). \end{aligned} \quad (13)$$

We define the m^{th} order polynomial and associated a_j coefficients as follows:

$$\begin{aligned} p_m(t) &= \sum_{j=0}^m a_j \varphi_j(t) \\ a_j &= (f, \varphi_j)/(\varphi_j, \varphi_j), \quad (j = 0, 1, \dots, m) \end{aligned} \quad (14)$$

The recursive definitions for the first and second derivatives are given respectively as:

$$\begin{aligned} \varphi'_i(t) &= \varphi'_{i-1}(t)(t - b_i) + \varphi_{i-1}(t) - c_i\varphi'_{i-2}(t) \quad (i \geq 1) \\ \varphi''_i(t) &= \varphi''_{i-1}(t)(t - b_i) + 2\varphi'_{i-1}(t) - c_i\varphi''_{i-2}(t) \quad (i \geq 2) \end{aligned} \quad (15)$$

Here the codes were developed in C/C++ which provides for recursive functions which we exploited for the evaluation of all the terms. The experimental data were fitted to an m^{th} order expression $\lambda_m(t)$ defined below

$$\lambda_m(t) = \sum_{j=0}^m h_j t^j = p_m(t) = \sum_{j=0}^m a_j \varphi_j(t) \quad (16)$$

The coefficients h_i are all computed recursively, and the derivatives determined from (16) or from (14) and (15). Once h_j or a_j are determined, then the gradient to the curve $\lambda_m(t)$ is computed as

$$\lambda'_m(t) = \sum_{j=0}^m j h_j t^{j-1}. \quad (17)$$

The $l_Q(t)$ function of (2) is expanded similarly as for $\lambda_m(t)$ for order m . The orthogonal polynomial method is stable and the mean square error decreases with higher polynomial order in general monotonically (where n is used to denote the integer order), but the differentials are not so stable, because of the contribution of higher order coefficients in the differential expression as will be shown. From the form of the equation that will be developed, the rate constant is determined as the gradient of a straight-line graph in the appropriate segment of the graph. However, the curvature

of the plot will increase with increasing n , giving a poorer value of k , whereas higher values of n would better fit the λ vs t curve. Hence inspection of the plots is necessary to decide on the appropriate n value, where we choose the lowest n value for the most linear graph of the expression under consideration that also provides a good $\lambda(t)$ fit over a suitable time range over which the k rate constants apply. The orthogonal polynomial stabilization method provides good λ fits with increasing n , but not gradients, so that the onset of sudden changes to the gradient which on physical grounds is unreasonable can be used as an indication as to which is the best curve to select. There is in practice little ambiguity in selecting the appropriate polynomials, as will be demonstrated. Reactions (i) and (ii) both gauge initial concentrations in terms of the A_∞ (λ_∞) or final reading of a physical factor proportional to concentration and the structure of the analysis is the same and will therefore be discussed simultaneously, followed by reactions (iii) to (iv), where concentrations are measured directly during the course of the reaction, which will be discussed together because the form of the boundary conditions and data are of the same class.

2 ANALYSIS OF REACTIONS (I) and (II)

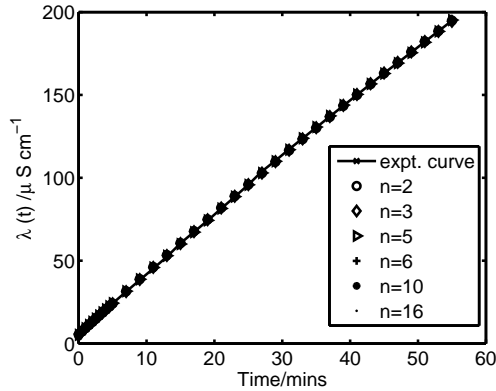


Figure 1: Plot of (i) using orthogonal polynomials for various orders n . The the least squares deviation goes down dramatically with increasing n , which was found not to be the case with the normal non-orthogonal polynomial method.

Figure (1) are plots for the different polynomial orders n for reaction (i). It will be noticed that higher n values in general leads to better fits visually; the normal least squares method leads to severe kinks and loop formation for $n \geq 4$ which is not evident here. The reaction (ii) data covers a far greater domain with respect to half-lifetimes with only about 14 points (which is a poor dataset with respect to our methods but which still gives quantitatively accurate values); because of the relatively more rapid curvature changes, we would expect very different gradient behavior as compared to (i) with its stronger linearity.

The corresponding plots for reaction (ii) are in Fig. (2).

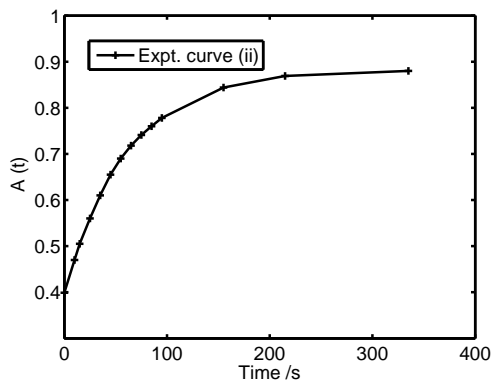


Figure 2: Experimental points omitting point at A_∞ for reaction (ii) at time = 2135s. The curve is rather non-linear.

In view of the nonlinearity, we chose a limited regime to curve fit for polynomial order $n = 3, 4, 5$ in Fig.(2) and the gradient was computed for the $n = 5$ polynomial to determine the rate constants as it was the only order that gave a smooth curve for the first 12 consecutive points in the range; the other orders also gave consistent and almost equal gradients except at the extreme end points of the range plotted as depicted for example in Figs. (6, 8, 12).

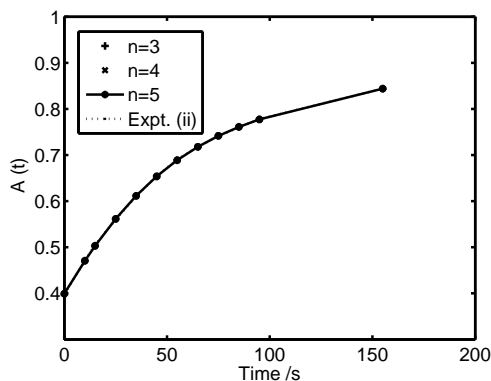


Figure 3: Experimental points curve fitted with polynomials of order $n = 3, 4, 5$. The fit for this range is excellent, despite the nonlinear nature of the curve

Unlike reaction (ii), the λ_∞ for reaction (i) was ambiguous. The plot of (10) was made for the same experimental values with different λ_∞ 's, both higher and lower than the supposed experimental value for this reaction. The plots in Fig.(4) shows increasing

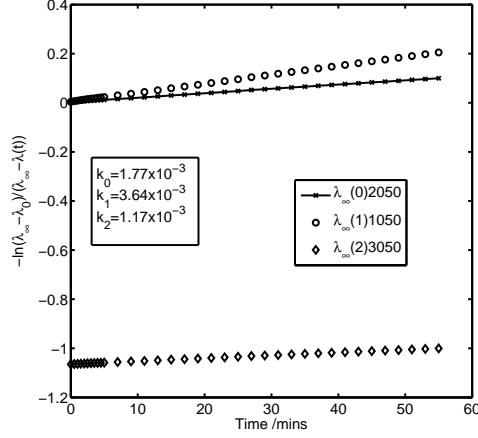


Figure 4: Integrated equation(10) plot with λ_∞ from experiment (0) and from two different arbitrary values (1,2) for λ_∞ , which yields two different values for the rate constant due to gradient change.

k_a for decreasing λ_∞ ; the choice $\lambda_\infty = 1050$ leads to a value of k_a close to the NLA values for the different methods discussed which does not require λ_∞ , but is also able to determine this value by extrapolation. The rate constant from NLA is higher than that determined from experiment, implying a lower λ_∞ value which is consonant with evaporation of solvent and/or the non-equilibration of temperature prior to measurement to determine λ_∞ . Hence elementary NLA allows one to deduce the accuracy of the actual experimental methodology in this example. Except for one section, we shall apply NLA based on constant k assumption. We also quote some values of Khan's results [20, Table 7.1] in Table (1), where some comment is required. The A absorbance is monotonically increasing and at higher time (t) values (see [20, Table 7.1]) the experimental A value exceeds the A_∞ that is determined by the process of minimizing $\sum d_i^2$. Hence the minimization of $\sum d_i^2$ with respect to A_∞ is taken as a protocol for determining the best k value even if it contradicts experimental observation. Further, this protocol is highly sensitive to A ; a change of 10^{-3} leads to an approximately ten-fold change in k . On the other hand, if A_∞ determined from experiment as 0.897 is accepted, then then computed rate constant for this value is $k = 2.69 \times 10^{-3} \text{s}^{-1}$ implying that the uncertainty in k is of the order of $\pm 14 \times 10^{-3}$. Hence we can conclude that the Khan method is a protocol that accepts as correct the k value that is determined by the minimization of A_∞ for a certain A_∞ range ($\approx 0.8980 - .8805$), which again refers to an unspecified protocol as to the choice of the range.

The general 1st and 2nd order equations We state the standard integrated forms below as a reference that requires specification of initial concentrations in order to contrast them to the methods developed here.

$10^3 \sum d_i^2$	513.5	109.4	8.563	63.26	212.7	227.4
A_∞	.8805	.881	.882	.883	.885	.887
$10^3 k/s^{-1}$	$19.7 \pm .6$	$18.1 \pm .3$	$16.5 \pm .1$	$15.5 \pm .2$	$14.2 \pm .4$	$13.3 \pm .5$

Table 1: Some results from reaction (ii) [20, p.381, Table 7.1]. The first row refers to the square difference summed, where the lowest value would in principle refer to the most accurate value (third entry from left). The second row refers to the A_∞ absorbance and the last to the corresponding rate constant with the most accurate believed at the stated units to be at $16.5 \pm .1$.

The first order rate constant k_1 is determined from

$$k_1 = \frac{1}{t} \log_e \{b(b-x)\} \quad (18)$$

and the second order rate constant k_2 is determined from

$$k_2 = \left[\frac{1}{t(a-b)} \right] \log_e \frac{b(a-x)}{(b-x)} \quad (19)$$

where these expressions are given in [23, p.2063] and utilized to compute rate constants where a and b are the initial concentration terms at $t = 0$ and x is the extent of reaction.

2.0.1 Method 1

This method is a variant of the direct method of eq.(2). For constant k , the rate equation $\frac{dc}{dt} = -kc = -k(a-x)$ reduces to

$$\frac{\lambda(t)}{dt} = -k\lambda(t) + \lambda_\infty \cdot k \quad (20)$$

Hence a plot of $\frac{\lambda(t)}{dt}$ vs $\lambda(t)$ would be linear. We find this to be the case for polynomial order $npoly \leq 3$ as in Fig.(5) below for all data values; higher polynomial orders can be used in selected data points of the curve below, especially in the central region. Thus criteria must be set up to determine the appropriate regime of data points for a particular polynomial order in NLA. For $n=2$, $k_a = 3.34 \pm .03 \times 10^{-3} \text{min}^{-1}$ and $\lambda_\infty = 1134 \pm 10$ units. The plots for reaction (ii) is a little more involved; it is a much more rapid reaction and the number of data-points are relatively sparse for NLA and the points cover the entire range of the reaction sequence and is highly non-linear; it was found that the gradients were smooth for the first 10 or so points and reasonably linear, but that at the boundary of these selected points, there are deflections in the curve; on the other hand, the different order polynomial curves ($n \leq 5$) are all coincident over a significant range of these values; we chose the $n = 5$ polynomial curve to determine the curve over the entire range and the linear least squares fit yields the following data $k_b = 1.64 \pm .04 \times 10^{-2} \text{s}^{-1}$ and $A_\infty = 0.8787 \pm .0008$ units.

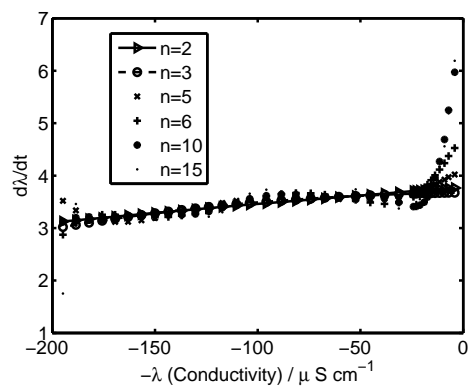


Figure 5: Method 1 graph showing linearity lower order polynomial fits for reaction (i).

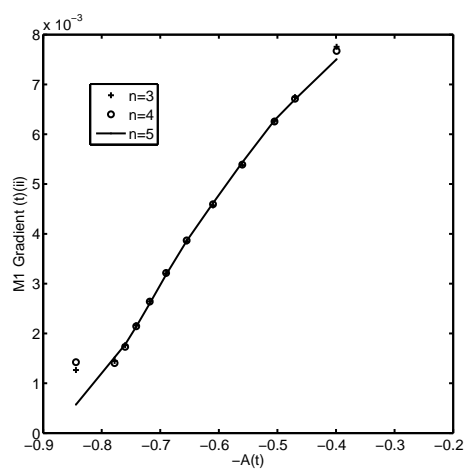


Figure 6: Method 1 applied to reaction (ii). Only at the peripheral value does the fit fail for lower values of n due to the extreme curvature.

2.0.2 Method 2

This method is yet another variant of the direct method of eq.(2). Let $\alpha' = \lambda_\infty - \lambda_0$, then $\ln \alpha' - \ln(\lambda_\infty - \lambda) = kt$, then noting this and differentiating yields

$$\underbrace{\ln \left(\frac{d\lambda}{dt} \right)}_Y = \underbrace{-kt}_{Mt} + \underbrace{\ln[k(\lambda_\infty - \lambda_0)]}_C \quad (21)$$

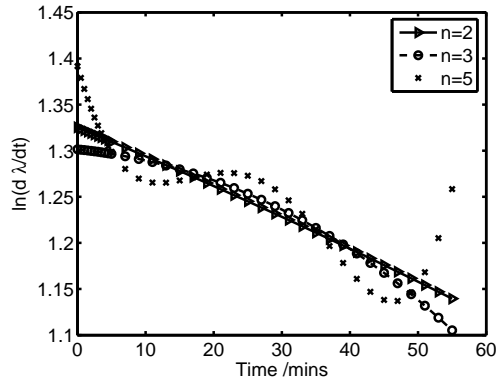


Figure 7: Method 2 reaction (i) where smooth curves are obtained for at least $npoly < 4$.

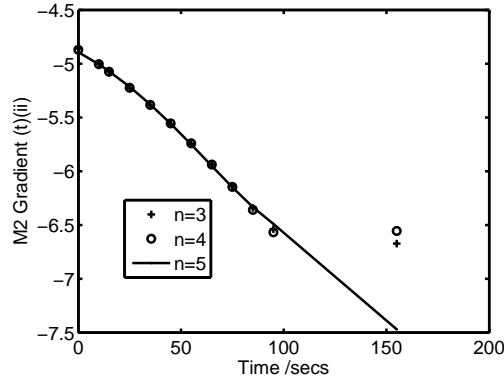


Figure 8: Method 2 reaction (ii) where smooth curves are obtained for $npoly < 5$. The $n = 5$ polynomial is used to calculate the best linear line over this range as the other polynomials do not fit for the last value in the series due to the extreme curvature.

A typical plot that can extract k as a linear plot of $\ln(d\lambda/dt)$ vs t is given in Fig.(7) for Method 2, reaction (i) and in Fig.(8) for Method 2, reaction (ii). Linearity is observed for $npoly = 2$ and smooth curves without oscillations for at least $npoly \leq 3$ for reaction (i) and an analysis for reaction (ii) uses $npoly = 5$. The linear least square line yields for Method 2 the following:

$$\begin{aligned} k_a &= 3.35 \pm .03 \times 10^{-3} \text{min}^{-1} \text{ and } \lambda_\infty = 1130 \pm 10 \text{ units} \\ k_b &= 1.72 \pm .02 \times 10^{-2} \text{s}^{-1} \text{ and } A_\infty = 0.86(53) \pm .02 \text{ units.} \end{aligned}$$

We note that because of the manifest nonlinearity of the gradients, one cannot determine the A_∞ values to 4-decimal place accuracy as quoted by Khan based on his model and assumptions [20, Table 7.1].

2.0.3 Other associated non-direct methods

There are other methods, one of which is a variant of Method 1 and another that utilizes a least-squares optimization of the form of the equation for first and second derivatives.

2.0.4 Method 1 variation

A variant method similar to the Guggenheim method [2] of elimination is given below but where gradients to the conductivity curve is required, and where the average over all pairs is required; the equation follows from (21).

$$\langle k \rangle = \frac{-2}{N(N-1)} \sum_i^N \sum_{j>i}^N \ln(\lambda'(t_i)/\lambda'(t_j)) / (t_i - t_j) \quad (22)$$

Since we are averaging over instantaneous k values, there would be a noticeable standard deviation in the results if the hypothesis of change of rate constant with species concentration is correct. Differentiating (21) for constant k leads to (23) expressed in two ways

$$\frac{d^2\lambda}{dt^2} = -k \left(\frac{d\lambda}{dt} \right) \quad (a) \text{ or } k = -\frac{d^2\lambda}{dt^2} / \left(\frac{d\lambda}{dt} \right) \quad (b) \quad (23)$$

If $\lambda(t) = \sum_{i=0}^{n+1} a(i)t^{i-1}$, then as $t \rightarrow 0$, the rate constant is given by $k = \frac{-2a(2)}{a(1)}$ from (23b). For the above, n , id , and iu denotes as usual the polynomial degree, the lower coordinate index and the upper index of consecutive coordinate points respectively, where the average is over the consecutive points, whereas the k rate constant with subscript "all" below refers to the equation (22).

The results from this calculation are as follows:

$$\begin{aligned} k_{a,all}, k_{a,id,iu} &= 3.32, 3.23 \pm .07 \times 10^{-3}, \text{min}^{-1}, n = 2, id = 10, iu = 20 \\ k_{a,t \rightarrow 0} &= 3.082 \times 10^{-3} \text{min}^{-1}. \\ k_{b,all}, k_{b,id,iu} &= 1.7150, 1.676 \pm .3 \times 10^{-2}, \text{s}^{-1}, n = 5, id = 1, iu = 10 \\ k_{b,t \rightarrow 0} &= 1.023 \times 10^{-2} \text{s}^{-1}. \end{aligned}$$

The asymptotic limit gives a lower value for k_b than for the other methods for reactions (i) and (ii). One possible explanation is that the rate constant changes as a function of time, but we note that (23) was derived assuming constant k .

2.0.5 Optimization of first and second derivative expressions

Eq.(23(b)) suggests another way of computing k for “well-behaved” values of the differentials, meaning regions where k would appear to be a reasonable constant. The (a) form suggests an exponential solution. Define $\frac{d\lambda}{dt} \equiv dl$ and $\frac{d^2\lambda}{dt^2} \equiv d^2l$. Then $dl(t) = A \exp(-kt)$ and $dl(0) = A = h_2$ from (16). Furthermore, as $t \rightarrow 0$, $k = (-2h_2/h_1)$ and a global definition of the rate constant becomes possible based on the total system $\lambda(t)$ curve.

With a slight change of notation, we now define dl and d^2l as referring to the continuous functions $dl(t) = A \exp(-kt)$ and $d^2l(t) = -kA \exp(-kt)$ and we consider $(d\lambda/dt)$ and $d^2\lambda/dt^2$ to belong to the values (16) derived from ls fitting where $(d\lambda/dt) = \lambda'_m$, $(d^2\lambda/dt^2) = \lambda''_m$ which are the experimental values for a curve fit of order m . From the experimentally derived gradients and differentials, we can define two non-negative functions $R_\alpha(k)$ and $R_\beta(k)$ as below:

$$\begin{aligned} R_\alpha(k) &= \sum_{i=1}^N \left(\frac{d^2\lambda(t_i)}{dt^2} + k dl(t_i) \right)^2 \\ R_\beta(k) &= \sum_{i=1}^N \left(\frac{d\lambda(t_i)}{dt} - dl(t_i) \right)^2 \end{aligned} \quad (24)$$

where

$$f_\alpha(k) = R'_\alpha(k) \quad \text{and} \quad f_\beta(k) = R'_\beta(k)$$

and a stationary point (minimum) exists at $f_\alpha(k) = f_\beta(k) = 0$. We solve the equations f_α , f_β for their roots in k using the Newton-Raphson method to compute the roots as the rate constants k_α and k_β for functions $f_\alpha(k)$ and $f_\beta(k)$ respectively. The error threshold in the Newton-Raphson method was set at $\epsilon = 1.0 \times 10^{-7}$. We provide a series of data of the form $[n, A, k_\alpha, k_\beta, \lambda_{\alpha,\infty}, \lambda_{\beta,\infty}]$ where n refers to the polynomial degree, A the initial value constant as above, k_α and k_β are the rate constants for the functions f_α and f_β (solved when the functions are zero respectively) and likewise for $\lambda_{\alpha,\infty}$ and $\lambda_{\beta,\infty}$. The e symbol refers to base 10 (decimal) exponents. The λ_∞ values are averaged over all the 36 data points for reaction (i) and for the 12 datapoints of reaction (ii) from the equation

$$\lambda_\infty = \frac{d\lambda(t)}{dt} \frac{1}{k} + \lambda(t) \quad (25)$$

for scheme α and β for both reaction (i) and (ii). The results are as follows.

Reaction (i)

$$\begin{aligned} &[2, 3.7632 \times 10^0, 3.2876 \times 10^{-3}, 3.2967 \times 10^{-3}, 1.1506 \times 10^3, 1.1477 \times 10^3], \\ &[3, 3.6384 \times 10^0, 2.7537 \times 10^{-3}, 2.7849 \times 10^{-3}, 1.34756 \times 10^3, 1.3334 \times 10^3], \\ &[4, 3.6384 \times 10^0, 2.0973 \times 10^{-3}, 2.4716 \times 10^{-3}, 1.7408 \times 10^3, 1.4900 \times 10^3], \\ &[5, 4.0213 \times 10^0, 9.7622 \times 10^{-3}, 4.9932 \times 10^{-3}, 4.4709 \times 10^2, 7.9328 \times 10^2], \\ &[6, 4.5260 \times 10^0, 4.1270 \times 10^{-2}, 8.9257 \times 10^{-3}, 1.7101 \times 10^2, 4.8403 \times 10^2]. \end{aligned}$$

We noticed as in the previous cases that the most linear values occur for $1 < n < 4$. In this approach, we can use the f_α and f_β function similarity of solution for k_α and k_β to determine the appropriate regime for a reasonable solution. Here, we notice a sudden departure of similar value between k_α and k_β (about 0.4 difference) at $n = 4$ and so

we conclude that the probable average “rate constant” is about the range given by the values spanning $n = 2$ and $n = 3$. Interestingly, the λ_∞ values are approximately similar to the ones for method 1 and 2 for polynomial order 2 and 3 for reaction (i). More study with reliable data needs to be done in order to discern and select appropriate criteria that can be applied to these non-linear methods. Because of the large number of datapoints in the linear range, k_a and k_b values are very compatible for $n = 2, 3$ where the k_a determination involves double derivatives, which cannot be determined with accuracy unless a sufficient number of points is used.

Reaction (ii)

The results for this system are

$$[5, 7.5045 \times 10^{-3}, 1.2855 \times 10^{-2}, 1.5497 \times 10^{-2}, .94352, .89247]$$

for the first 12 datapoints of the published data to time coordinate 155 secs. For polynomial order 3,4 and the first 11 datapoints, where there are no singularities in the curve we have

$$[3, 7.7275 \times 10^{-3}, 1.4469 \times 10^{-2}, 1.6147 \times 10^{-2}, .91320, .88335]$$

$$[4, 7.4989 \times 10^{-3}, 1.3146 \times 10^{-2}, 1.5359 \times 10^{-2}, .94208, .89652].$$

Here, k_a and k_b differ by $\sim .2 \times 10^2 \text{s}^{-1}$; one possible reason for this discrepancy is the insufficient number of datapoints to accurately determine $\frac{d^2\lambda}{dt^2}$. Even if the number of points are large, experimental fluctuations would induce changes in the second derivative which would be one reason for discrepancies. Hence experimentalists who wish to employ NLA must provide more experimental points, especially at the linear region of the $\lambda(t)$ vs t curve.

2.1 Inverse Calculation

Rarely are experimental curves compared with the ones that must obtain from the kinetic calculations. Since the kinetic data is the ultimate basis for deciding on values of the kinetic parameters, replotting the curves with the calculated parameters to obtain the most fitting curve to experiment would serve as one method to determine the best method amongst several. For reaction (i) we have the following data:

Result	Procedure	Poly. order	λ_∞	k_a
1	From expt	-	2050.	1.7752×10^{-3}
2	Method 1	2	1134.3	3.3397×10^{-3}
3	Method 2	2	1130.23	3.347×10^{-3}
4	sec(2.0.5) R_α	2	1150.63	3.288×10^{-3}

Table 2: Data for the plot of Fig.(9) for reaction(i)

For reaction(ii), we have the following:

Fig.(9) indicate that the parameters derived from experiment is the worst fit compared to the methods developed here, verifying that our computations, including the λ_∞ values are a better fit than the one derived from experiment due to flaws in the methodology of driving the reaction to completion by heating, leading to evaporation

Result	Procedure	Poly. order	λ_∞	k_a
1	From expt	-	.8820	1.65×10^{-2}
2	Method 1	5	.8787	1.64×10^{-2}
3	Method 2	5	.8653	1.72×10^{-2}
4	$\sec(2.0.5) R_\beta$	5	.89247	1.5497×10^{-2}

Table 3: Data for the plot of Fig.(10) for reaction (ii).

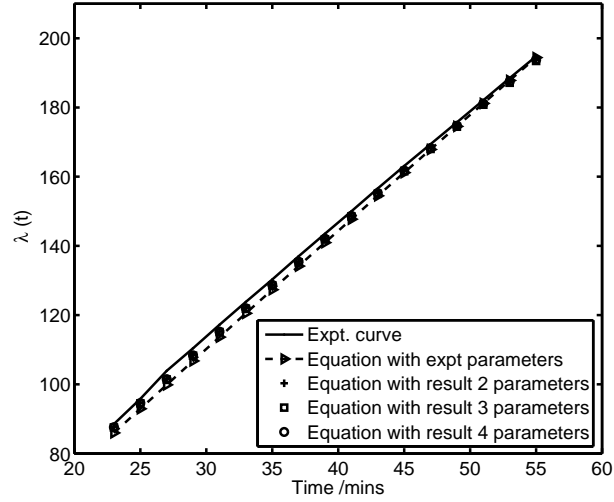


Figure 9: The plots according to the k_b and A_{ifity} values of Table(2)

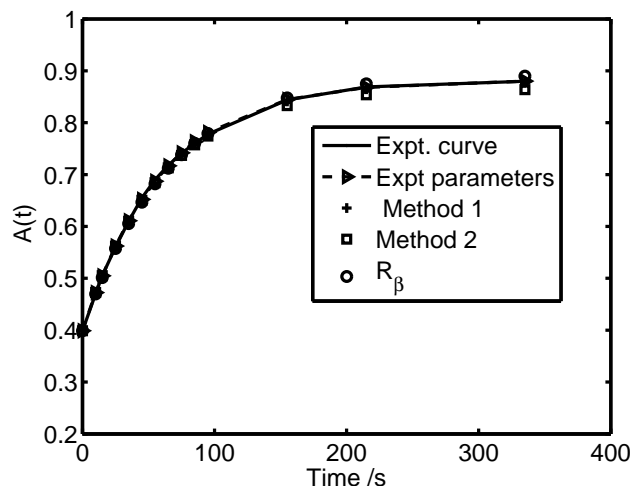


Figure 10: The plots according to the k_b and A_{inf} values of Table(3)

and therefore inaccurate determination. Based on the comparisons between the reactions (i) and (ii), we predict that reaction (i) if carried out under stringently controlled conditions, especially in determining λ_∞ would have a rate constant approximately $\sim 3.2 \times 10^{-3} \text{ mins}^{-1}$ rather than the experimentally deduced $\sim 1.77 \times 10^{-3} \text{ mins}^{-1}$ with $\lambda_\infty \sim 1130$ units rather than 2050 units. For reaction (ii), we note a good fit for all the curves, that of the experiment, Khan's results and ours.

2.2 Evidence of varying kinetic coefficient k for reactions (i) and (ii)

Finally, what of direct methods that do not assume the constancy of k which was the case in the above subsections? Under the linearity assumption $x = \alpha\lambda(t)$, the rate law has the form $dc/dt = -k(t)(a - x)$ where $k(t)$ is the instantaneous rate constant and this form implies

$$k(t) = \frac{d\lambda/dt}{(\lambda_\infty - \lambda(t))} \quad (26)$$

If λ_∞ is known from accurate experiments or from our computed estimates, then $k(t)$ is determined; the variation of $k(t)$ could provide crucial information concerning reaction kinetic mechanism and energetics, from at least one theory recently developed for elementary reactions [13] *at equilibrium*; and for such similar theories [24] and experimental developments for very large changes in concentration, it may be anticipated that nonlinear methods would be used to accurately determine $k(t)$ that would yield the so-called "reactivity coefficients" [13] that account for variations in k that would provide fundamental information concerning activation and free energy changes. However, since these coefficients pertain to the steady-state scenario where a precise relationship

exists between the ratio of these coefficients and that of the activity, one might not expect to detect these coefficients for relatively minute concentration changes that occur in most routine chemical reaction determinations. On the other hand, the very preliminary results here seem to indicate transient variations belonging possibly to another class of phenomena ; it could well be due to periodicity in the reactions where some of the "beats" detected -assuming no experimental error in the data- could be related to the time interval between measurements, that is, because the number of datapoints is restricted, only certain beats are observed in the periodicity. The assumption that the spectroscopic detector is not noisy relative to the magnitude of the experimental data and that it does not have significant periodic drift relative to a reference absorbance leads to the conclusion that some form of chemically induced periodicity might be present. It would be very interesting to increase the number of datapoints where the time interval between measurements is reduced and to analyze the different types of apparent frequencies that might be observed with different time intervals of measurement. From these observations, perhaps theories could be adduced on the nature of these presumed fluctuations.

Reaction (i) results

Figure(11) refers to the computations under the assumption of first order linearity of concentration and the conductivity. Whilst very preliminary, non-constancy of the rate constants are evident, and one can therefore expect that another area of fruitful experimental and theoretical development can be expected from these results that incorporates at least these two effects.

Reaction (ii) results

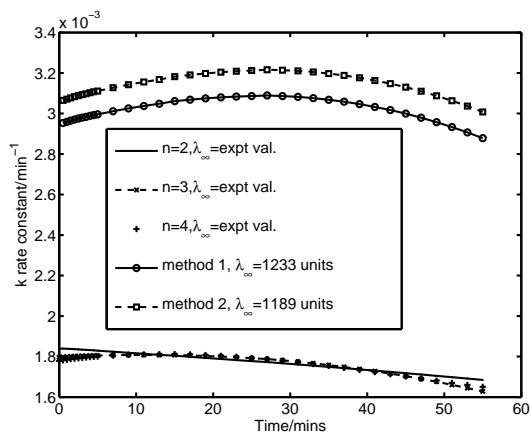


Figure 11: Variation of k with time or concentration changes based on the experimental value $\lambda_{\infty} = 2050$ units and the computations based on different polynomial degrees $n = 2, 3, 4$ and the computed λ_{∞} values for Method 1 and Method 2 for fixed polynomial degree $n = 3$.

To verify that the curious results are not due to minute fluctuations of the gradient,

we plot the gradient $\frac{dI}{dt}$ of the curve fits for polynomial orders 1, 2, 4 and 5. Even for low orders, the fit is very good with no oscillations observed between lower and higher order polynomials for approximately the first 10 values of the kinetic data in Fig.(12). It was found that the lower order polynomials gave essentially the same results for the restricted domain where the gradients coincided with those of higher order.

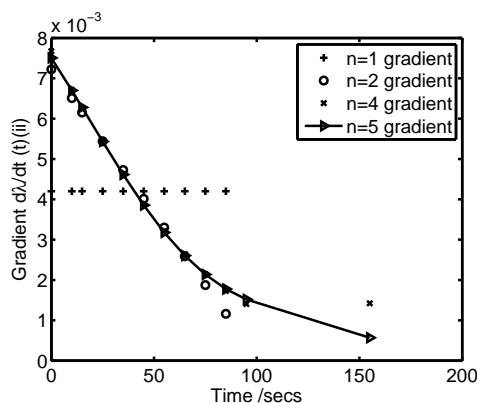


Figure 12: Variation of gradient $d\lambda = dt = dA/dt$ with time for different polynomial orders $n = 1, 2, 4$ and 5

The gradient drops to 0 at the long time $t \rightarrow \infty$ limit; on the other hand, the factor $\frac{1}{(\lambda_\infty - \lambda(t))}$ rises to infinity; so we might expect from these two competing factors various sinusoidal-like properties, or even maxima. The surprising result is shown in Fig. (13). It could be that the form (26) is not valid because no instantaneous value of the rate constant can be defined. Also, it is not possible at this stage to definitively rule out the detector causing a sinusoidal variation due to periodic drift and instability. On the other hand, if we can rule out artifacts due to systematic instrument error, then one must admit the possibility that a long-time cooperative effect involving coupling of the reactant molecules through the solvent matrix over the entire reaction chamber may take place. This seems like a big idea that could be investigated further. However, if the results are due solely to instrument error, then this method allows us to monitor the error fluctuations by taking a suitable weighted average. We note that reaction (ii) is relatively complex, involving many ionic species and some intermediate steps or reactions [20, p.414-416]. This fact, coupled with the cell setup where steady state temperature gradients might well exist, would lead to coupled processes described by irreversible thermodynamics, which could possibly explain such rate constant changes relative to the first order parametrization used here.

Comment: Barring artifacts, Figs.(11-13) is consonant with two separate effects: (α) a long-time limit due to changes in concentration that alters the force fields and consequently the mean rate constant value (according to the theories in [13, 24]) of the reaction as equilibrium is reached, and (β) possible transient effects due to collective modes of the coupling between the reacting molecules and the bulk solution as observed in the region between the start of the reaction and the long-time interval. In

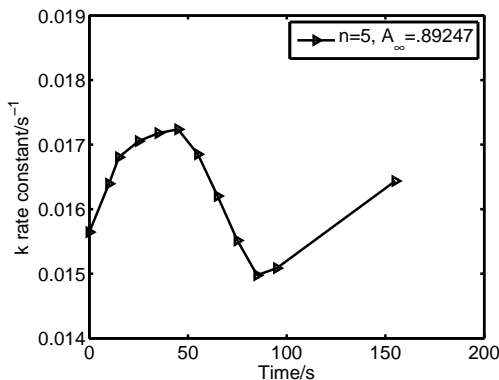


Figure 13: An apparently periodically varying rate constant that settles to a higher value at larger time increments. A_{∞} was the value taken from Method 1 above for polynomial order 5.

both reactions (i) and (ii), there appears a slight change in the rate constant value at time $t = 0$ and the values at the end of the experimental measured interval which may be due to the altered force fields that would change slightly the rate constant according to (α) . On the other hand, there is a relatively slow and minute sinusoidal-like change in the rate constant that may be due to some cooperative effect, if no artifacts are implied; the interpolation with different polynomials leading to the same gradient seems to suggest that some type of collective behavior might be operating during the course of the reaction; if this is so then (β) would be a new type of phenomena that has not hitherto been incorporated into chemical kinetics research.

3 RESULTS FOR REACTION (III) and (IV)

Two different methods are utilized to determine the reaction rate constants. The direct method utilizes determining the gradient k of the $d[A_1]/dt$ vs $[Q]$ curve of eq.(2) by fitting the best straight line. Initial concentrations are not required, and the error in the gradient may be estimated from the mean least squares error of the end-points; define the mean square per point Δ^2 as $\Delta^2 = \sum_{i=1}^n (\bar{y} - y_i)^2 / 2$ where \bar{y} is the linear optimized curve and y_i a datapoint within the range of measurement. Then for the range of datapoints $|X| = |Q|$ we estimate the error in the rate constant as $\Delta k = \sqrt{\Delta^2} / |X|$. For what follows below the first order rate constant for reaction (iii) is denoted k_{1d} derived from direct computation of the gradient of (2) whereas k_{1ls} denotes the rate constant as calculated by our least squares method (5). Similarly, for reaction (iv), k_{2d} denotes the rate constant derived directly from the gradient of the curve following eq.(2) by fitting the best straight line and k_{2ls} is the second order rate constant from the *least squares minimization* of (5). A detailed description follows below.

3.1 Reaction (iii) first order details

Fig.(14) is a plot of the various orthogonal polynomial order fits. The $n = 2$ order is rather poor but higher orders all coincide with the experimental points. And for $n > 2$, we find that the gradient curves coincide within a certain range where $[A] > 0.005\text{M}$. If in fact the order is 1 or unity, a plot of $[\dot{A}]$ vs $[A]$ would be entirely linear. Fig. (15) depict these plots, where some linearity is observed for $[A] > 0.005\text{M}$.

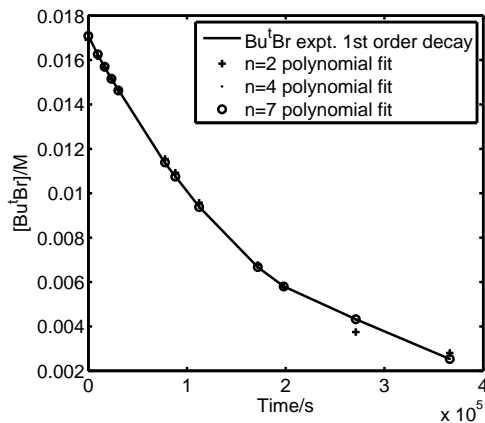


Figure 14: The polynomial degree n for the orthogonal polynomial fit for the first order Bu^tCl reaction (iii) where there is near coincidence for $n = 4, 5, 6, 7$.

Fig.(15) shows a coincidence of the rate curves for order $n = 5-7$ above $[A]=0.005\text{M}$. It may be therefore inferred that for at least $n > 5$, and for $[A] > 0.005\text{M}$, the gradient represents the rate constant. The inaccuracy for very low concentrations may be explained by reference to Fig.(14). The experimental curve is parametrized as

$$[A] = \sum_{i=1}^{n_r} h_i t^i \quad (27)$$

The time parameter is very large at low concentrations ($> 3.5 \times 10^5\text{s}$) of Bu^tBr ; the h_i values would be small and the uncertainties in the reactant concentration relatively high; this explains the large scatter in the gradient values at low concentrations. We therefore ignore the first two values of $[A]$ at low concentrations and focus on the gradients for points of coincidence of the different polynomial curves in in Fig.(15). The results are shown in Table 4. The linear fit in this specified range yields k_{1d} . The absolute root mean squared deviation per datapoint of Fig.(14) is listed in the last rhs column of Table 4 where the best fit is in the range $n = 5 - 7$. The average k_{1d} value taking into account the error estimate is $(5.4 \pm 0.5) \times 10^{-6}\text{s}^{-1}$. which is close to the $(5.22 \pm 0.3) \times 10^{-6}\text{s}^{-1}$ of the experimentalists. For the same regime

The results from the literature for this first order reaction [25, Table IX,p.2071] using equation (18) has a mean value of 5.22×10^{-6} and for the 12 datapoints determined

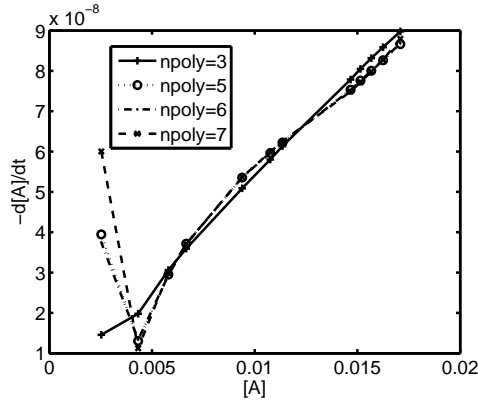


Figure 15: A plot of the rate of decomposition of $\text{Bu}^t\text{Br} (\equiv \text{A})$ vs A where $[\text{A}]$ refers to the molar concentration of Bu^tBr according to the kinetic data published in [25, Table IX.] for reaction (iii).

n	k_{1d}/s^{-1}	k_{1ls}/s^{-1}	Est. error in k	Abs. Dev. in n
2	5.038689×10^{-6}	4.881742×10^{-6}	4.164406×10^{-7}	0.000151
3	5.374684×10^{-6}	5.307609×10^{-6}	8.129860×10^{-8}	0.000073
4	5.053045×10^{-6}	5.047342×10^{-6}	3.541633×10^{-7}	0.000034
5	5.398782×10^{-6}	5.181527×10^{-6}	2.772767×10^{-7}	0.000014
6	5.393767×10^{-6}	5.184763×10^{-6}	2.723767×10^{-7}	0.000013
7	5.500610×10^{-6}	5.187774×10^{-6}	3.028407×10^{-7}	0.000014

Table 4: Results for the first order Bu^tBr reaction neglecting last datapoint for calculating the mean rate constant k .

, and this value of k varied with range $(5.04 - 5.48) \times 10^{-6}$ in appropriate dimensions. The results as computed according our methods in Table 4 Table 4 shows the absolute deviation per point to be quite small, and Fig.(14) shows some plots. The gradient of the curves are graphed for various n in Fig.(15). The linear fit in this specified range yields k_{1d} . The absolute root mean squared deviation per datapoint of Fig.(14) is listed in the last rhs column of Table 4 where the best fit is in the range $n = 5 - 7$. The average k_{1d} value taking into account the error estimate is $(5.4 \pm 0.5) \times 10^{-6} \text{s}^{-1}$ which is close to the $(5.22 \pm 0.3) \times 10^{-6} \text{s}^{-1}$ of the experimentalists. For the same regime, (5) is used to compute k_{1ls} listed in the 3rd column. For $n = 5 - 7$, $k_{1s} = 5.18 \times 10^{-6} \text{s}^{-1}$ which is exceptionally close to the experimental determination mentioned above based on the integrated equation (18). requiring initial concentrations.

Lastly, (3) is used to compute the instantaneous rate constant shown in Fig.(16). We note that a maximum is formed before a drop at lower concentrations. Again, the concave form with a maximum is evident here as for reactions (i)-(ii).

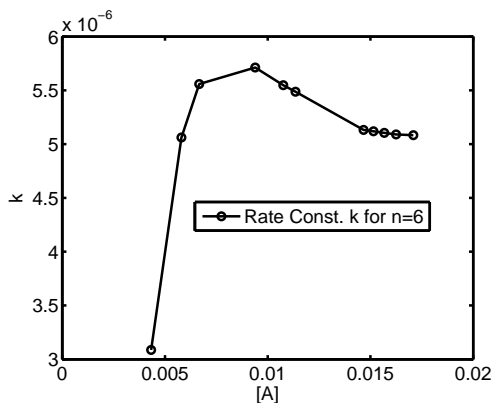


Figure 16: The direct calculation of the change of the rate constant with concentration $[A]=[Bu^tBr]$ directly from the published experimental data [25, Table IX.] for reaction (iii).

3.2 Reaction (iv) second order details

The pioneer experimentalists had decided *a priori* that the NaOEt iso-PropylBr (Pr^iBr) was second order and therefore did not independently measure the NaOEt and the Pr^iBr concentrations as shown in Fig.(18). Such a setting introduces a larger degree of scattering even if the rate order is known *a priori* to be the appropriate one; the scattering becomes evident in the rate constant curve of Fig.(21). The orthogonal polynomial fit is very good for $n > 3$ in Fig.(18). The gradient curve of Fig.(19) shows a coincidence of points for polynomial order $n > 3$ except for the measurement at the lowest concentrations, for the same reasons as given for reaction (iii). Fig. (20) is a close-up of the rate *vs* $[A][B]$ curve where the first 2 points show significant scatter. We ignore the first 3 points of lowest concentrations in our calculations for k_{2d} and k_{2ls} for different polynomial orders n ; k_{2d} is the rate constant by linear least squares fit to each of the curves of Fig. (19) of $d[A]/dt$ *vs* $[A][B]$ for different polynomial orders n and k_{2ls} is the rate constant calculated according to (5). The results are presented in Table 5. In Table 5, the value of k_{2d} is remarkably constant for $n = 4$ to 7, in keeping with the curves of Fig. (19) that are coincident for the selected concentration ranges where we have $k_{2d} = (2.80 \pm .07) \times 10^{-6} M^{-1} s^{-1}$ which is very close also to the computed k_{2ls} values, where the average value may be written $k_{2ls} = (2.83 \pm .05) \times 10^{-6} M^{-1} s^{-1}$.

The experimental results for this second order reaction [23, Table VII,p.2064] using equation (19) has a mean value of $2.88 \times 10^{-6} M^{-1} s^{-1}$ ($2.95 \times 10^{-6} M^{-1} s^{-1}$ if solvent expansion is taken into account according to an extraneous theory), and for the 19 data-points determined, k varied within the range $(2.76 - 2.96) \times 10^{-6} M^{-1} s^{-1}$. Fig.(21) graphs the instantaneous rate constant for reaction (iv) for the concentration ranges used for calculating k_{2d} and k_{2ls} . Again a semi-sinusoidal shaped curve is observed. There is evident scatter in this graph which may be attributed to the fact that $[A]$ and $[B]$ are completely correlated and there is no possibility of random cancellations due to

independent measurement of both $[A]$ and $[B]$. The form of the curve is as for reaction (iii) in Fig.(16) *and* as for reaction (ii) in Fig.(13) if we ignore the low concentration value as having a large scatter at about $t = 150$ s. Even the ambiguous reaction (i) shows a shallow concave shape, as with all the rest. Fig.(17) is a pallet for the 4 diverse reactions (i)-(iv) of different orders reported by different sources all depicting the same general form; suggestive of some type of overall "chemical inertia" effect. The data for reaction (ii) were determined over 50 years apart from (iii) and (iv) by prominent persons, especially Ingold and co-workers who were amongst the best kineticists of the 20th century, apart from elucidating and defining the SN1, SN2, E1 and E2 reactions in organic chemistry. It seems that all these reactions depict a transient and long-ranging coupling phenomena hitherto unnoticed due to traditional analysis that uses integrated rate law expressions with the presupposition of invariant rate constants, which is also built into current statistical mechanics theories. There could be at least two separate possibilities:

(a) independently of the initial concentrations, one observes a rise in the rate constant before falling when the reactant concentration falls. Hence if we started a reaction at the midpoint concentrations close to the peak rate constant value in the reaction runs for reactions (ii)-(iv), then the rate constant profile will show a form similar to those shown here, except the peak rate constant will shift to lower concentrations, at least at a concentration less than the concentration at the commencement of the reaction. This possibility suggests some type of "chemical momentum" which is a long-ranging coupling phenomena that current statistical mechanical theories are not able to account for. Obviously this scenario admits the possibility of hysteresis behavior

(b) the rate constant is simply a function of reactant and product concentrations as outlined for instance in [13] and no hysteresis behavior exists.

Currently, mainstream statistical mechanical theories do not have a quantum or classical description of (a) and (b) above.

Reality would probably be described by broadly either (a) or (b) above with a possibility of the other playing a minor role in the contributed effect.

More careful experiments under stringent conditions need to be performed to :

- α . verify the existence of this effect by using other methods just in case the polynomial method has a property that induces a maximum in the gradient at approximately the midpoint of the domain range under investigation
- β . determine which of the two (a) or (b) above is the preponderant effect.

4 CONCLUSIONS

The differential methods developed here yield results for the average rate constant that is consistent and close in value to the traditional integrated law expression for 3 reactions whose rate constants were determined with precision by reliable and prominent kineticists, implying that the methods developed here are robust. Based on reproducibility of the method in relation to the standard protocol, we further test the differential methods for the ambiguous reaction (i) with regard to the inaccurate total reactant concentration (reflected in λ_∞) and we showed that the rate constant can

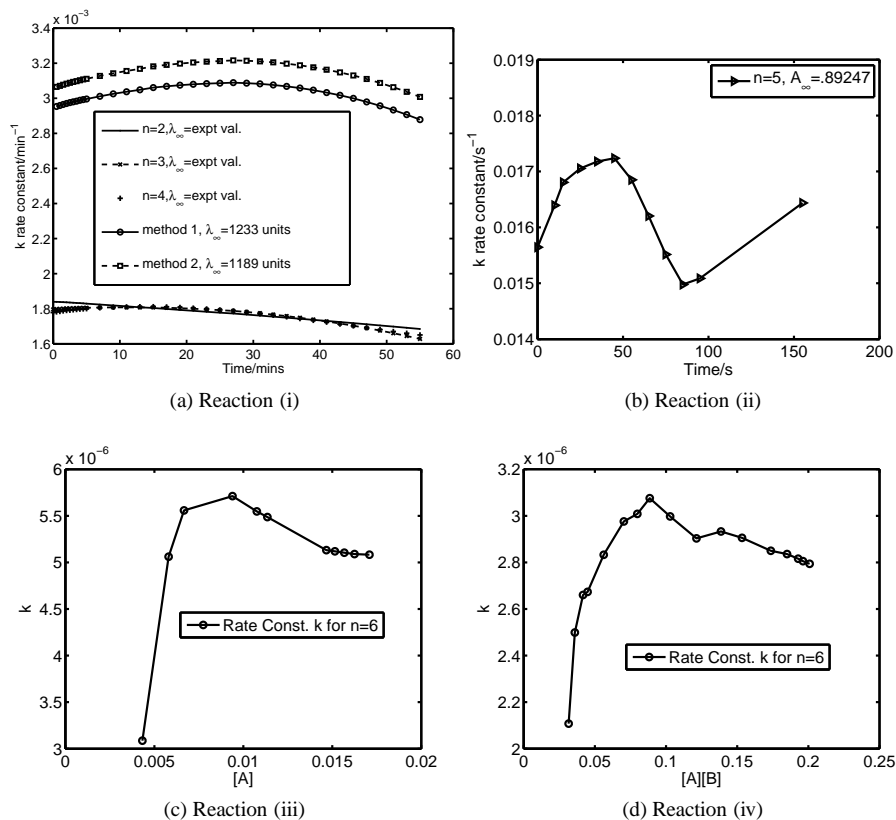


Figure 17: Collation of change of rate constants with concentration and time for reactions (i) to (iv).

n	$k_{2d}/\text{M}^{-1}\text{s}^{-1}$	Error Δk_{2d}	$k_{2ls}/\text{M}^{-1}\text{s}^{-1}$
2	1.251043×10^{-6}	1.189216×10^{-7}	2.180891×10^{-6}
3	2.142702×10^{-6}	8.845014×10^{-8}	2.654936×10^{-6}
4	2.818337×10^{-6}	6.850636×10^{-8}	2.829915×10^{-6}
5	2.822939×10^{-6}	6.600369×10^{-8}	2.833440×10^{-6}
6	2.876573×10^{-6}	6.613089×10^{-8}	2.853618×10^{-6}
7	2.770475×10^{-6}	7.707235×10^{-8}	2.823186×10^{-6}

Table 5: Results for the second order $\text{Pr}^i\text{Br} - \text{NaOEt}$ reaction neglecting the last 3 data-points that are discontinuous for calculating the rate constants k_{2d} and k_{2ls} .

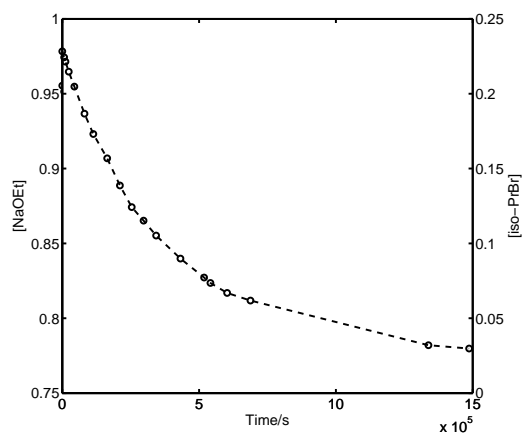


Figure 18: The experimental decay curve for the NaOEt iso-PropylBr (Pr^iBr) reaction [23, Table VII,p.2064] for reaction(iv).

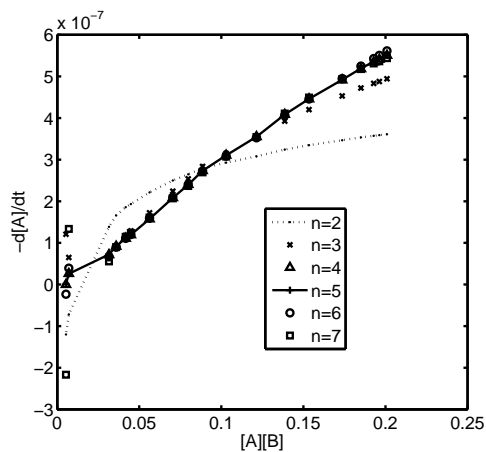


Figure 19: The rate curve shows that the polynomial order $n=2-3$ is too low to fit the changes of gradient. The other curves of higher order all coincide exactly for very large time values or low reactant concentrations. The average gradient is calculated by ignoring these values that are off-scale. $[\text{A}] \equiv [\text{NaOEt}]$ and $[\text{B}] \equiv [\text{iso-PropylBr}]$ in Molar concentration units.

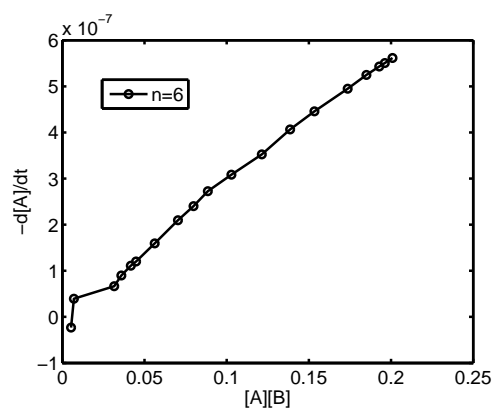


Figure 20: Close-up of the rate curve with reactant product concentration. The last 3 lowest product concentration points are ignored in the rate averaging to determine the rate constant.

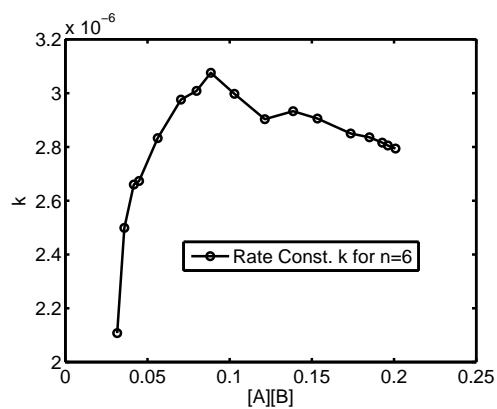


Figure 21: The computation of the instantaneous rate along the regime of coincidence of the polynomials for $n = 4 - 7$ for $n = 6$.

be determined without such data. Since much science refers to systems whose key variables are not controllable, as in astrophysical measurements and in forensics and archaeological studies, these methods could prove useful for analysis in these areas for reactions to arbitrary order.

All the reactions studied with different orders and mechanisms within the polynomial optimization method all show some type of "chemical rate constant momentum" effect in that there is a gradual acceleration in the rate over time initially followed by a sharp decrease as reactants depleted. This observation appears to be novel. Two independent factors might contribute to this effect: (A.) the transient coupling of thermodynamical force gradients with flows and species concentrations and molecular orientation that leads to the observed profile

(B.) the rate constant is a second order function of the reactant and product concentration according to [13]. That theory was based on evidence from *equilibrium* MD simulation of a chemical reaction.

Stringently controlled repeated experimentation is required to determine the relative contributions of (A.) and (B.) above. If a semi-sinusoidal profile is observed for different initial concentrations that covers the range of the concentration profile of a reference reaction of exactly the same type which also exhibits a semi-sinusoidal profile, then (A.) is the predominant mechanism which exhibits hysteresis behavior, whereas if the resulting profile of the experiments leads to a truncated semi-sinusoidal curve of the reference profile beginning at the initial concentration of the experimental run, the (B.) is the major effect. There is of course the possibility of a combination of effects (A.) and (B.) to varying degrees. Both effects have not been anticipated in current kinetic theories, which implies that these effects in themselves constitutes one area for further investigation.

Whilst the main purpose of this work is not to provide physical explanations, we suggest that the resulting curves in Figs.(17) can be explained by introducing X contributing factors or processes in real time. The first (f1) involves the fact that the reactants are initially separated, and the molecules must diffuse homogeneously before they can begin to interact. The second process (f2) involves reactant interaction with the solvent matrix, which would impede the reactive interactions and also conceivably raise the activation energy relative to unbounded reactants and lastly (f3) describes the product solvent matrix interaction, which is probably is not too significant for the typical reactions studied here. At the initial stage of the reaction, there is minimal solvent reactant interaction which would result in the caging of the reaction active sites and so the reaction is diffusion limiting; within a certain time scale, the mutual diffusion of reactants would allow for more reactant-reactant interactions, leading to an apparent increase in the rate constant; with the progress in time, however, the caging of reactants due to (f2) would increase the effective activation energy and hence lower the value of the rate constant which explains the precipitous drop at large time values; process (f3) might prevent in some cases the back reaction due to the breakup of the product to reactant molecules, and it may moderate (f2) by limiting the number of active solvent interaction with the reactant molecules. One might expect (f1) to cause the rise in the rate constant, and (f2) the lowering, leading to the concave maximum observed in all the reactions due to these competing processes. Conventional kinetics, modeled after ideal situations of homogeneity, is not able to account for these fine second order

details in the change in the reaction rate. Even in the homogeneous case, such as a reactive system in thermodynamical equilibrium, it was found that the rate constant is a well-defined function of the reactant and product concentrations, but this contribution to the changes found here is probably of second order for the typical reactions mentioned here.

The results presented here provides alternative developments based on NLA that is able to probe into the finer details of kinetic phenomena than what the standard representations allow for, especially in the the areas of changes of the rate constant with the reaction environment as well as determine average rate constant values without λ_∞ being known. Even with the assumption of invariance of k , one can always choose the best type of polynomial order that is consistent with the assumption, and it appears that the initial concentration as well as the rate constant seems be predicted as global properties based on the polynomial expansion. It should be noted that the examples chosen here were first order ones; the methods are general and they pertain to any form of rate law where the gradients and forms can be curve-fitted and the form of the equations optimized as in section (2.0.5). One other research area that may be investigated is the possibility of reactions of fractional order; elementary reactions are by nature of integer order; is there a method that can reduce them to fractional order if the rate constant is indeed in part a weak function of the reactant concentrations?

5 ACKNOWLEDGMENTS

This work was supported by University of Malaya Grant UMRG(RG077/09AFR) and Malaysian Government grant FRGS(FP084/2010A).

BIBLIOGRAPHY

1. P. Moore. Analysis of kinetic data for a first-order reaction with unknown initial and final readings by the method of non-linear least squares. *J. Chem. Soc., Faraday Trans. I*, 68:1890–1893, 1972.
2. E. A. Guggenheim. On the determination of the velocity constant of a unimolecular reaction. *Philos Mag J Sci*, 2:538–543, 1926.
3. W.D. Johnson and M.C. Maltby. The application of polynomial expressions to determine the initial concentrations and rate constants of chemical reactions. *Aust. J. Chem.*, 24:2417–2420, 1971.
4. E. S. Swinbourne. Method for obtaining the rate coefficient and final concentration of a first-order reaction. *J. Chem. Soc.*, 473:2371–2372, 1960.
5. E. S. Swinbourne. Determination of the rate coefficient and final concentration of a reaction of order n . *Aust. J. Chem.*, 16(1):170–173, 1963.

6. R.C. Williams and J.M. Taylor. Computer calculations of first-order rate constants. *J. Chem. Educ.*, 47(2):129–133, 1970.
7. N. H. Lajis and M. N. Khan. Kinetic demonstration of chemospecific reactions involving salicylate esters and amines. *J. Chem. Educ.*, 70(10):A264–A271, 1993.
8. M. J. J. Holt and A. C. Norris. A new approach to the analysis of first-order kinetic data. *J. Chem. Educ.*, 54(7):426–428, 1977.
9. W. E. Wentworth. Rigorous least squares adjustment . Application to some non-linear equations,II. *J. Chem. Educ.*, 42(3):162–167, 1965.
10. W. E. Wentworth. Rigorous least squares adjustment . Application to some non-linear equations,I. *J. Chem. Educ.*, 42(2):96–103, 1965.
11. J. J. Houser. Estimation of a_{∞} in reaction-rate studies. *J. Chem. Educ.*, 59(9):776–777, 1982.
12. J. E. Cortés-Figueroa and D. A. Moore. Using a graphing calculator to determine a first-order rate constant when the infinity reading is unknown. *J. Chem. Educ.*, 79(12):1462–1464, 2002.
13. C. G. Jesudason. The form of the rate constant for elementary reactions at equilibrium from md: framework and proposals for thermokinetics. *J. Math . Chem*, 43:976–1023, 2008.
14. K.B. Wiberg. Use of computers. In Edward S. Lewis, editor, *Techniques Of Chemistry*, volume VI of *Investigation of rates and mechanisms of reactions*, chapter XIII, pages 741–776. Wiley-Interscience, 1974. Part 1 General considerations and Reactions at Conventional Rates.
15. D.F. De Tar. Lskin1. In Delos F. De Tar, editor, *Computer Programs for Chemistry*, volume I, chapter 6, page 126. W. A. Benjamin, New York and Amsterdam, 1969. Fortran Program listing with brief theoretical explanation.
16. Delos F. Detar. LSKIN2. In Delos F. Detar, editor, *Computer Programs for Chemistry*, volume 4, chapter 1, page 1. Academic Press, New York and London, 1972. The chapter describes a method based on expansion of integrated rate equations for second order reactions that give estimates of the rate constant and initial concentrations.
17. X. Zhang, J. M. Ajello, and Y. L. Yung. Atomic carbon in the upper atmosphere of Titan. *Astrophys J*, 708:L18–L21, 2010.
18. M. B. McElroy and J. C. McConnell. Atomic carbon in the atmospheres of Mars and Venus. *J. Geophys. Res.*, 76(28):6674–6690, 1971.
19. C. A. Barth, C.W. Hord, J. B. Pearce, K. K. Kelly, G. P. Anderson, and A.I. Stewart. Mariner 6 and 7 ultraviolet spectrometer experiment: upper atmospheric data. *J. Geophys. Res*, 76:2213–2217, 1971.

20. Mohammad Niyaz Khan. *MICELLAR CATALYSIS*, volume 133 of *Surfactant Science Series*. Taylor & Francis, Boca Raton, 2007. Series Editor Arthur T. Hubbard.
21. S. Yakowitz and F. Szidarovsky. *An Introduction to Numerical Computations* . Maxwell Macmillan, New York, 1990.
22. W.H. Press, S.A. Teukolsky, W.T. Vetterling, and B.P. Flannery. *Numerical Recipes in C -The Art of Scientific Computing*. Cambridge University Press, second edition, 2002.
23. M. L. Dhar, E. D. Hughes, and C. K. Ingold. 420. Mechanism of elimination reactions. Part X. Kinetics of olefin elimination from isopropyl, sec.-butyl, 2-n-amyl, and 3-n-amyl bromides in acidic and alkaline alcoholic media. *J. Chem Soc.*, pages 2058–2065, 1948.
24. C. G. Jesudason. An energy interconversion principle applied in reaction dynamics for the determination of equilibrium standard states. *J. Math. Chem. (JOMC)*, 39(1):201–230, 2006.
25. M. L. Dhar, E. D. Hughes, and C. K. Ingold. 421. Mechanism of elimination reactions. Part XI. Kinetics of olefin elimination from tert.-butyl and tert.-amyl bromides in acidic and alkaline alcoholic media. *J. Chem Soc.*, pages 2065–2072, 1948.